International Journal of Automotive Technology, Vol. 18, No. 1, pp. 69−77 (2017)
DOI 10.1007/s12239−017−0007−7

pISSN 1229−9138/ eISSN 1976−3832

INTELLIGENT ALGORITHM BASED ON SUPPORT VECTOR DATA DESCRIPTION FOR AUTOMOTIVE COLLISION AVOIDANCE SYSTEM

I. B. YANG[1, 2)], S. G. NA[2)] and H. HEO[2)*]

[1)]Department of Smart Automobile, Soonchunhyang University, Chungnam 31538, Korea
[2)]Department of Control and Instrumentation Engineering, Korea University, Seoul 02841, Korea

(Received 10 October 2014; Revised 22 June 2015; Accepted 9 July 2016)

ABSTRACT−This paper presents a theoretical expansion of a new intelligent algorithm called extended support vector data description (E-SVDD) for the analysis and control of dynamic groups to realize macroscopic and microscopic behavior prediction in an automotive collision avoidance system. The time to collision concept was extracted as a key parameter via system modeling and used with the E-SVDD algorithm to set up the relevant generalized theoretical system. A new method, along with its practical application, to predict the behavior of micro- and macro-systems in real time and improve the control logic for collision avoidance was realized. A numerical simulation based on actual driving data was performed to compare the proposed collision avoidance logic and the conventional one. The results confirmed the improved performance and effectiveness of the proposed control logic.

KEY WORDS : E-SVDD (Extended-Support Vector Data Description), Automotive collision avoidance system, TTC (Time to Collision), Automotive control logic

1. INTRODUCTION

Many dynamic systems are exposed to various irregular disturbances such as atmospheric turbulence and road surfaces. Many real systems also experience regular disturbances.

Dynamic systems for cases such as traffic flows of vehicles and pedestrians are associated with many dynamic targets operating independently under finite spatiotemporal conditions.

A dynamic group consists of elements that move independently within the group in a limited time and space frame. It often needs to be controlled in order to avoid any possible collision. Examples of dynamic groups include a group of cars on a road or crowd of people moving somewhere. Such a system contains several dynamic elements governed by Newtonian mechanics; it has certain patterns with behavioral uncertainty. Some features need to be applied to the control and analysis of systems because of the effect of coupling (Jansson, 2004). These dynamic elements are characterized by their mutual interconnectedness and coupling in a simultaneous manner. Accordingly, a method for proper analysis of the situation is indispensable. It is necessary to ensure precise analysis and stable control techniques for a dynamic group having simultaneous interconnectedness and unpredictability. A new logic is needed that enables macroscopic prediction (i.e., recognition of situation) and microscopic prediction (i.e., searching and tracking). To guarantee the control stability and accuracy for the control and analysis of systems with simultaneous connectivity and irregular disturbance, a new control strategy and logic are needed to recognize a situation and trace/observe simultaneously.

Various sensors have been used in mechatronics-based complex machine systems such as cars and robots to determine the external surroundings. More precise behavior prediction techniques via more efficient decision logic are necessary (Prosser, 2007; Schneider, 2005; Blum and Eskandarian, 2002; Oh *et al*., 2008; Han, 2013; Jeong *et al*., 2012; Jung *et al*., 2010; Oh *et al*., 2009). The range of detection can be drastically expanded via a communication network–based sensing system. Nevertheless, this approach has limited applicability to most dynamic systems because of problems with effectiveness and standardization.

In this study, a theory was developed for the analysis of the microscopic and macroscopic behavior of a group of cars, and a new warning logic to protect against collision is proposed. A simulation was conducted to verify the feasibility and compare the performance with that of a conventional method.

This paper is organized as follows. Section 2 describes the target system and the modeling method and introduces conventional collision avoidance algorithms. Section 3 presents the proposed vehicle collision avoidance system warning logic. Section 4 presents the simulation of the proposed logic based on actual driving data. Section 5

**Corresponding author.* e-mail: heo257@korea.ac.kr

compares the proposed logic with a conventional logic. Finally, section 6 presents the concluding remarks.

2. COLLISION AVOIDANCE THEOREM AND LOGICS

This section presents vehicle interaction modeling and conventional collision avoidance logic. Newtonian mechanics is applied to moving objects, and a modeling technique is used to describe the unpredictability, interconnectedness, and random environment in terms of the relative velocity and distance.

Table 1 defines modeling variables for the interaction between the following and preceding vehicles in the target vehicle system.

In Figure 1, the following and preceding vehicles are represented as FV and PV, respectively. Subscripts f and p are also used in this paper to represent the following and preceding vehicles, respectively. The modeling variables can be classified according to two bases: the absolute (X_f, X_p, V_f, V_p, A_f, A_p) and relative (X_r, V_r, A_r) motion of vehicles.

The time to collision (TTC) was a key parameter in this study and can be defined in terms of variables that represent relative motion. TTC is defined in Equation (1) using the distance between vehicles and the relative velocity:

$$TTC = -\frac{X_p - X_f}{V_p - V_f} = -\frac{X_r}{V_r} \tag{1}$$

Table 1. Variables in modeling.

Variables	Description	Unit
X_f	Moving distance of following vehicle	m
X_p	Moving distance of preceding vehicle	m
X_r	Relative distance between following vehicle and preceding vehicle	m
V_f	Velocity of following vehicle	km/h
V_p	Velocity of preceding vehicle	km/h
V_r	Relative velocity between following vehicle and preceding vehicle	km/h
A_f	Acceleration of following vehicle	m/s^2
A_p	Acceleration of preceding vehicle	m/s^2
A_r	Relative acceleration between following vehicle and preceding vehicle	m/s^2

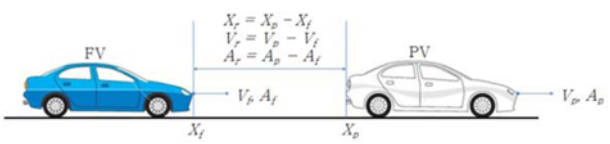

Figure 1. Description of modeling variables.

A smaller TTC represents a dangerous situation with the risk of collision. However, the TTC defined in Equation (1) does not consider the acceleration relative to the following vehicles; thus, its accuracy is lower in cases involving relative acceleration. Thus, the parameter TTCa, which considers the acceleration, should be defined as follows:

$$\begin{aligned} X_r(\Delta t) &= X_r(0) + \int_0^{\Delta t} V_r(t)dt \\ &= X_r(0) + V_r(0)\Delta t + \frac{1}{2}A_r\Delta t^2 \end{aligned} \tag{2}$$

Equation (2) represents the distance between vehicles after Δt. TTCa is defined as the time when the distance between vehicles is 0:

$$X_r(0) + V_r(0)(TTCa) + \frac{1}{2}A_r(TTCa)^2 = 0 \tag{3}$$

Equation (3) can be rearranged to redefine TTCa in the following Equation (4):

$$TTCa = \frac{-V_r(0) + \sqrt{V_r(0)^2 + 2X_r(0)A_r}}{A_r} \tag{4}$$

The simple logic A, which is a conventional warning logic, is explained below (Butsuen *et al*., 1994). $X_{braking}$ represents the decreasing distance between the preceding and following vehicles under maximum braking conditions, as shown in Equation (5). When the distance between vehicles is less than $X_{braking}$, a warning signal is given.

$$X_{braking} = \frac{1}{2}\left(\frac{V_f^2}{A_f} - \frac{V_p^2}{A_p}\right) + V_f\tau_{hum} + V_r\tau_{sys} + X_{min} \tag{5}$$

where A_f and A_p are the maximum decelerations of the following and preceding vehicles, respectively, and τ_{hum} and τ_{sys} are the response delays of the driver and system, respectively, and X_{min} is headway offset (minimum headway distance when the vehicle stops against the preceding vehicle). This logic A is complemented with conventional logic B, for which the model is as follows (Seiler *et al*., 1998):

$$\begin{aligned} X_w &= \frac{1}{2}\left(\frac{V_f^2}{A_f} - \frac{(V_f - V_r)^2}{A_f}\right) + V_f(\tau_{sys} + \tau_{hum}) + X_{min} \\ X_{br} &= V_r(\tau_{sys} + \tau_{hum}) + \frac{1}{2}A_f(\tau_{sys} + \tau_{hum})^2 \end{aligned} \tag{6}$$

where X_w is the distance for pre-warning and X_{br} is the distance for emergency warning.

Logic B provides a pre-warning and emergency warning when the distances between vehicles are less than X_w and X_{br}, respectively. This logic has warning systems that combine the sensitive pre-warning and insensitive emergency warning according to the traffic conditions. Advantages of this logic include the ease of setting parameters and the low complexity. However, this logic

has the drawback of frequent inaccurate warnings on the driver. Hence, an intelligent collision avoidance logic that regulates warnings under microscopic and macroscopic conditions is presented in the following section.

3. INTELLIGENT COLLISION AVOIDANCE LOGIC

This section introduces the intelligent algorithm called extended support vector data description (E-SVDD), which is applied in the proposed intelligent collision avoidance algorithm to recognize the condition of the following vehicle. E-SVDD is an extension of SVDD, which is used for pattern recognition. First, SVDD is introduced. Second, the intelligent behavior estimation algorithm with E-SVDD is described. The recognition of vehicles around the following vehicle and the risk correlation map are also explained.

3.1. SVDD Technique

SVDD is a well-known one-class support vector learning method used for pattern recognition. It uses a sphere in feature space to classify normal data in abnormal data (Tax and Duin, 2004).

SVDD approximates the support of data in a normal region as follows:

Consider a sphere B with a center at $a \in R^d$ and radius R having a dataset D. Some of the learning data may be abnormal due to sensitivity to noise. The main objective of the SVDD method is to collect as much learning data in the smallest sphere possible.

The sphere that satisfies the SVDD objective can be obtained by solving the following optimal problem:

$$\begin{aligned} &\min L_0(R^2, a, \zeta) = R^2 + C\sum_{i=1}^{N} \zeta_i \\ &s.t. \|x_i - a\|^2 \le R^2 + \zeta_i,\ \ \zeta_i \ge 0,\ \ i = 1, \ldots, N. \end{aligned} \tag{7}$$

The variable ζ_i in Equation (7) is a penalty associated with the i-th learning data outside sphere. The objective function of Equation (7) consists of two opposing elements: The square of the radius R^2 and summation of penalties $\sum_{i=1}^{N} \zeta_i$. The tradeoff constant C adjusts the degree of importance between the two contradictory elements.

Equation (8) can be obtained by solving the optimal problem of Equation (7) by using the Lagrange function, dual problem, and kernel trick:

$$\begin{aligned} &\min_a \sum_{i=1}^{N}\sum_{j=1}^{N} \beta_i\beta_j\langle z_i, z_j\rangle - \sum_{i=1}^{N} \beta_i\langle z_i, z_i\rangle \\ &s.t. \sum_{i=1}^{N} \beta_i = 1,\ \ \beta_i \in [0, C],\ \ \forall i. \end{aligned} \tag{8}$$

Equation (8) is a quadratic problem. The variable β_i can be obtained with MATLAB by using the function "quadprog." The saddle-point condition that satisfies the optimal solution of the Lagrange function in the input space is given in the following Equation (9):

$$a = \sum_{i=1}^{N} \beta_i z_i \tag{9}$$

Because the distances between the means of each support vector x_i at the decision boundary and sphere center a is the radius of the sphere, the square of the radius R^2 can be obtained as shown in Equation (10).

$$\begin{aligned} &R^2 - \|z - a\|^2 = 0 \\ &R^2 - \left(\langle z, z\rangle - 2\sum_{i=1}^{N} \beta_i\langle z_i, z\rangle + \sum_{i=1}^{N}\sum_{j=1}^{N} \beta_i\beta_j\langle z_i, z_j\rangle\right) = 0 \end{aligned} \tag{10}$$

The normality of the test data x in the input space can be determined by using R^2 from Equation (10); hence, the decision function can be expressed as given in Equation (11) (Park *et al*., 2003; Duda *et al*., 2012; Na *et al.*, 2014).

$$\begin{aligned} \tilde{f}(z) &= R^2 - \|z - a\|^2 \\ &= R^2 - \left(\langle z, z\rangle - 2\sum_{i=1}^{N} \beta_i\langle z_i, z\rangle \right. \\ &\quad \left. + \sum_{i=1}^{N}\sum_{j=1}^{N} \beta_i\beta_j\langle z_i, z_j\rangle\right) \ge 0 \end{aligned} \tag{11}$$

When the SVDD method detects the normality of the data, it generates a sphere by finding the boundary solution to the optimal problem. Because the sphere can be simply represented by two parameters – the center and radius – it can be compared and analyzed with other datasets (Park and Leem, 2003, Park *et al*., 2007; Ypma *et al*., 1999; Yang, 2012). Thus the risk correlation between vehicles in a group in traffic can be generated in terms of the sphere obtained using the above SVDD method.

Based on the above SVDD concept, the procedure to establish the risk correlation between the following and preceding vehicles is as follows.

By mapping the distance data between the preceding and following vehicles on a two-dimensional plane, the sphere containing these data can be found via the SVDD method. The final value of the risk correlation for the following vehicle can be calculated by using the radius of the sphere after substituting the value for the sphere center to the risk correlation map. Figure 2 illustrates the concept of the procedure.

The above risk correlation method based on SVDD can be used to compensate for the conventional algorithm.

3.2. E-SVDD

The E-SVDD concept was implemented to estimate the risk correlation between the following vehicle and surrounding vehicles. The implementation procedure is as follows. Each center of the SVDD spheres can be found by

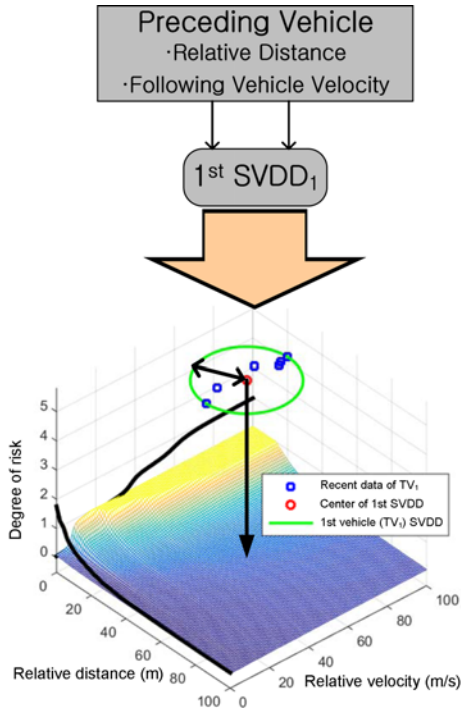

Figure 2. Conceptual diagram of risk correlation with preceding vehicle using SVDD technique.

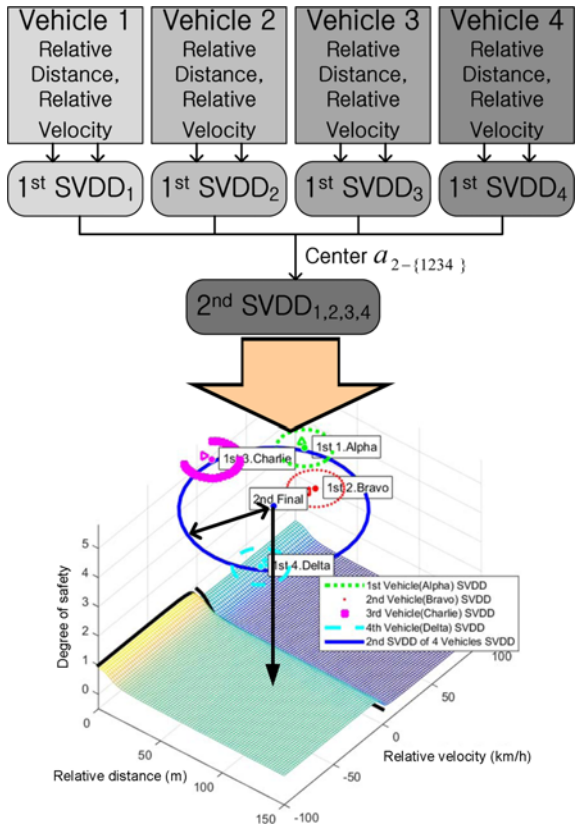

Figure 3. Conceptual diagram of risk correlation with surrounding vehicles using E-SVDD technique.

using the relative velocity and distance data of the surrounding vehicles.

A larger spherical boundary containing the centers of each sphere can also be generated via the SVDD method. The risk correlation with the surrounding vehicles is calculated by using the change and movement in the size of the extended sphere.

Figure 3 shows the E-SVDD method to generate the sphere and risk correlation when there are four surrounding vehicles.

3.3. Situation Prediction Theory

The situations of the preceding and surrounding vehicles are predicted simultaneously. First, the situation of the preceding vehicle is predicted by using the change in size of the sphere generated by SVDD and the corresponding value in the risk correlation map for the sphere center. Second, the situation of the surrounding vehicles is predicted by using the most recent data on the relative distances and velocities between following and surrounding vehicles except for the oncoming ones. If four surrounding vehicles, including the preceding one, are adopted in the analysis, the experimental formula to select the target vehicle (TV) is given in the following Equation (12):

$$\begin{aligned} &\mathrm{TV}_1\text{: } \min\left(C^{\mathrm{X}} \times \sqrt{(X_{\mathrm{r}} \cdot \sin\theta_{\mathrm{r}})^2} + X_{\mathrm{r}} \cos\theta_{\mathrm{r}}\right) \\ &\mathrm{TV}_2\text{: } \min(X_{\mathrm{r}} + C^{\mathrm{V}} \cdot V_{\mathrm{r}}) \\ &\mathrm{TV}_3\text{: } \min(X_{\mathrm{r}} + C^{\mathrm{V}} \cdot V_{\mathrm{r}}) \\ &\mathrm{TV}_4\text{: } \min\left(X_{\mathrm{r}} \times C^{\mathrm{W}} \cdot V_{\mathrm{r}} + \sqrt{(X_{\mathrm{r}} \cdot \sin\theta_{\mathrm{r}})^2}\right) \end{aligned} \tag{12}$$

where θ_{r} is the angle between the following and preceding vehicles; X_{r} is the relative distance (m); V_{r} is the relative velocity (km/h); C^{X} is the weighting factor to select the vehicle closest to the same lane as the first target vehicle (TV_1), where a larger value means that a vehicle with a smaller angle along the forward direction is chosen; and C^{V} is the weighting factor to select the second and third target vehicles (TV_2, TV_3) depending on the importance of the relative distance and velocity. A smaller value means a closer vehicle; a larger value means a vehicle with a faster closing velocity. C^{W} is also the weighting factor to select the fourth target vehicle (TV_4).

$C^{\mathrm{X}} = 50$, $C^{\mathrm{V}} = 0.5$ s and $C^{\mathrm{W}} = 1$ s are chosen by trial and error, and Equation (12) is experimentally obtained. Using Equation (12) above, excluding preceding vehicle TV_1 and among surrounding vehicles TV_2, TV_3, TV_4 fast approaching vehicle changing lane can be selected as target vehicle TV_4.

The data of the target vehicles obtained from Equation (12) are used as inputs for the SVDD and E-SVDD algorithms to calculate the risk correlation of the following vehicle with the preceding and surrounding ones. Figure 5 shows a schematic diagram of how to obtain the risk correlation between the situations of the preceding and surrounding vehicles via E-SVDD (Yang, 2012).

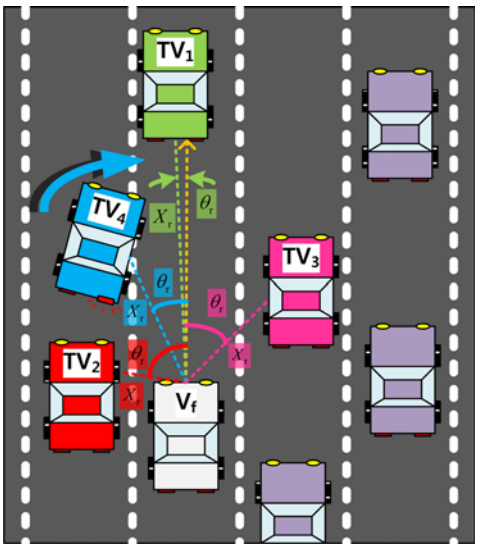

Figure 4. Selection of 4 Target Vehicles (TVs).

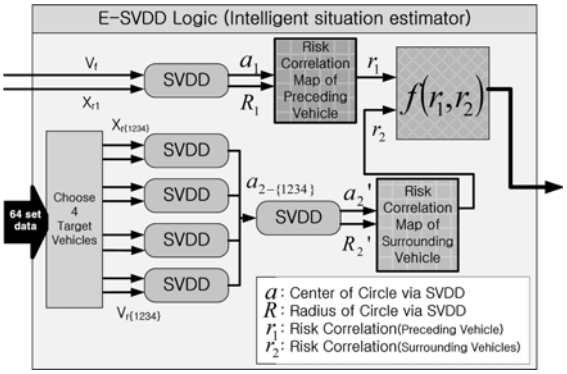

Figure 5. Intelligent prediction procedure for situations of preceding and surrounding vehicles via E-SVDD.

3.4. Generation of Risk Correlation Map

The proposed risk correlation maps are classified into those with preceding vehicles and those with surrounding vehicles. Both risk correlation maps utilize the relative distances between the preceding and following vehicles and the relative velocities between the surrounding and following vehicles. The degree of risk correlation number is between 0 and 1.

To represent the continuous variable of the risk correlation, the Cauchy cumulative distribution (CCD) which is intuitively easy in manipulation and adjustment of waveform was adopted, as shown in Equation (13):

$$\mathrm{CCD} = \frac{1}{\pi}\arctan\left(\frac{x-x_0}{\gamma}\right) + \frac{1}{2} \tag{13}$$

where x_0 is a parameter specifying the location of the peak of the distribution and γ is a scale parameter that specifies the half-width at half-maximum (HWHM) (Wikipedia, 2013).

On the risk correlation map with the preceding vehicle, the z axis represents the numerical risk correlation at (x, y). The x axis represents the risk distribution of the following vehicle with the preceding one. A shorter relative distance between them means a higher risk; this is formulated below as Equation (14):

$$\begin{aligned}
x_{x1} &= 1-\left(\frac{1}{\pi}\right)\cdot\arctan\left(\frac{X_r-X_{01}}{\gamma_{x1}}\right)-\frac{1}{2}\\
x_{x2} &= 1-\left(\frac{1}{\pi}\right)\cdot\arctan\left(\frac{X_r-X_{02}}{\gamma_{x2}}\right)-\frac{1}{2}\\
x_{x3} &= 1-\left(\frac{1}{\pi}\right)\cdot\arctan\left(\frac{X_r-X_{03}}{\gamma_{x3}}\right)-\frac{1}{2}\\
x_{x4} &= 1-\left(\frac{1}{\pi}\right)\cdot\arctan\left(\frac{X_r-X_{04}}{\gamma_{x4}}\right)-\frac{1}{2}\\
x_{x_f} &= 0.5\cdot x_{x1} + 0.4\cdot x_{x2} + 0.55\cdot x_{x3} + 0.55\cdot x_{x4}
\end{aligned} \tag{14}$$

where X_r is the relative distance (m) and $\mathbf{X}_{\{01,02,03,04\}}$ is a location parameter to control the position of the CCD. In addition, $X_{01} = 1$ m, $X_{02} = 5$ m, $X_{03} = 8$ m, and $X_{04} = 19$ m are selected via experiments.

$\gamma_{\{x1,x2,x3,x4\}}$ is a scale parameter to control the HWHM in the CCD. $\gamma_{x1} = 0.4$ m, $\gamma_{x2} = 0.9$ m, $\gamma_{x3} = 4$ m, and $\gamma_{x4} = 9$ m are also selected.

The eight experimentally obtained parameters of $X_{\{01,02,03,04\}}$, $\gamma_{\{x1,x2,x3,x4\}}$ determine the slopes and distributions of the contours with respect to the distance and corresponding x axis in the risk correlation map. x_{x_f} can be obtained by adding the previously derived weighting factors of 0.5, 0.4, 0.55, and 0.55 to $X_{\{x1,x2,x3,x4\}}$. The weighting factors can be adjusted by trial and error; this produces the contour forms in Figure 5.

The y axis in the risk correlation map with the preceding vehicle represents the risk distribution of the following vehicle with the preceding vehicle. A slower relative velocity between them means a higher risk; this is formulated below as Equation (15):

$$\begin{aligned}
y_{v1} &= \frac{1}{\pi}\cdot\arctan\left(\frac{V_f-V_{01}}{\gamma_{v1}}\right)+\frac{1}{2}\\
y_{v2} &= \frac{1}{\pi}\cdot\arctan\left(\frac{V_f-V_{02}}{\gamma_{v2}}\right)+\frac{1}{2}\\
y_{v3} &= \frac{1}{\pi}\cdot\arctan\left(\frac{V_f-V_{03}}{\gamma_{v3}}\right)+\frac{1}{2}\\
y_{v4} &= \frac{1}{\pi}\cdot\arctan\left(\frac{V_f-V_{04}}{\gamma_{v4}}\right)+\frac{1}{2}\\
y_{v_f} &= 0.5\cdot y_{v1} + 0.4\cdot y_{v2} + 0.55\cdot y_{v3} + 0.55\cdot y_{v4}
\end{aligned} \tag{15}$$

where V_f is the velocity of test vehicle.

$V_{\{01,02,03,04\}}$ are the location parameters to control the position of the CCD; the values are set to $V_{01} = 8$, $V_{02} = 5$, $V_{03} = 38$, and $V_{04} = 60$ km/h. $\gamma_{\{v1,v2,v3,v4\}}$ are scale parameters to control the HWHM of the CCD; the values are set to γ_{01}

= 1, γ_{02} = 1.2, γ_{03} = 3, and γ_{04} = 6. The eight experimentally obtained parameters of $V_{\{01,02,03,04\}}$, $\gamma_{\{v1,v2,v3,v4\}}$ determine the slopes and distribution of the contour with respect to the distance and corresponding y axis in the risk correlation map. y_{v_f} can be obtained by adding the previously derived weighting factors of 0.5, 0.4, 0.55, and 0.55 to $y_{\{v1,v2,v3,v4\}}$. The weighting factors can be adjusted by trial and error to make the contour forms shown in Figure 5. The risk correlation with respect to the relative distance and velocity of the test vehicle can be measured by multiplying the previously obtained x_{x_f} and y_{v_f}.

The risk correlation with the preceding vehicle can be numerically quantified as the multiplication of the risk correlation values for the corresponding situation on the x and y axes. Figure 6 illustrates the risk correlation map of the following vehicle with the preceding vehicle.

The measured risk correlation is a continuous number between 0 and 1; it represents greater danger when its numerical value is close to 1.

The risk correlation with the surrounding vehicles can also be represented along the x and y axes. The degrees of risk correlation in the corresponding situation (x, y) are shown in terms of the degree of darkness, which is regarded as the z axis.

The x axis represents the degree of risk correlation of the following vehicle depending on the relative distance between each surrounding vehicle. A shorter distance means a higher degree of risk correlation. The relevant logic is formulated below in Equation (16):

$$x_{x5} = 1 - \frac{1}{\pi} \cdot \arctan\left(\frac{X_r - X_{05}}{\gamma_{x5}}\right) - \frac{1}{2} \tag{16}$$

where X_r is the relative distance between the surrounding and following vehicles; the location parameter X_{05} = 10 m and scale parameter γ_{x5} = 5 of the CCD are experimentally determined.

In the risk correlation map, the y axis represents the risk distribution of the following vehicle with the surrounding vehicles. A smaller relative velocity between them means a higher degree of risk correlation; this is formulated below in Equation (17):

$$y_{v5} = 1 - \frac{1}{\pi} \cdot \arctan\left(\frac{V_r - V_{05}}{\gamma_{v5}}\right) - \frac{1}{2} \tag{17}$$

where V_r is the relative velocity between the following and surrounding vehicles; again, the location parameter V_{05} = −1 and scale parameter γ_{v5} = 2 of the CCD are experimentally determined.

The risk correlation with the surrounding vehicles can be defined as the summation of x_{x5} and y_{v5} divided by 2. Figure 7 illustrates the risk correlation map of the following vehicle with the surrounding vehicle. A shorter relative distance means a higher degree of risk correlation.

The final form of the intelligent collision avoidance logic is formulated by combining the above situation prediction algorithm using E-SVDD logic with the conventional logic B presented in Section 2. Figure 8 shows the details.

The risk correlation index α is calculated from the E-SVDD algorithm as an integer within [−3, 3]. The index α becomes an integer within [0, 2] via the normalization process. The normalized E-SVDD risk correlation is then

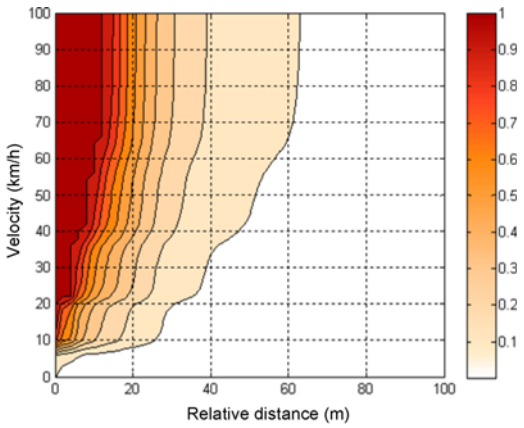

Figure 6. Risk correlation map with preceding vehicle.

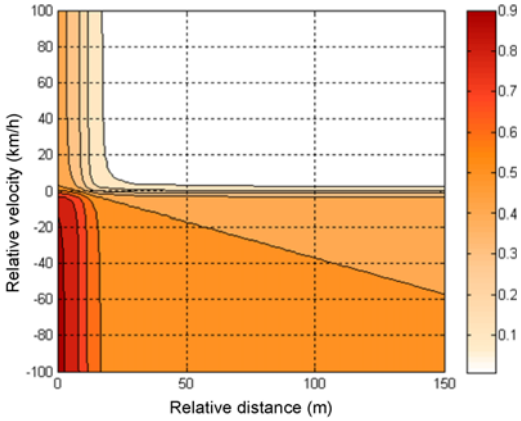

Figure 7. Risk correlation map with surrounding vehicle.

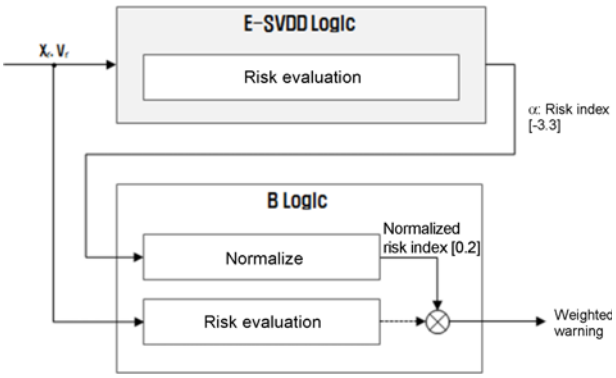

Figure 8. Schematics of intelligent collision avoidance system logic.

applied as a weight for the collision risk calculated from logic B.

The normalized risk correlation using E-SVDD for the weight is implemented as follows in Equation (18):

$$\hat{X}_{w} = X_{w} f(\alpha)$$
$$\hat{X}_{br} = X_{br} f(\alpha) \quad (18)$$

X_w and X_{br} are the warning distances estimated by Equation (14) in logic B. $f(\alpha)$ denotes a normalized risk index based on intelligent E-SVDD logic. Hence, a lower normalized risk correlation index means that X_w and X_{br} become smaller, which reduces the sensitivity of the warning signal. In contrast, a higher normalized risk correlation index means that X_w and X_{br} become larger, which increases the sensitivity of the warning signal. If the risk correlation approaches zero, this means that the warning distance has become zero. This results in no warning signal in any situation. The intelligent logic was simulated using MATLAB/Simulink (Yang, 2012).

4. SIMULATION

Numerical simulations integrating logic B and the proposed intelligent logic were conducted based on actual driving data. Using actual driving data from highway and urban roads as input to the proposed logic enabled its verification under actual traffic conditions. The sensor information was used as input in the collision avoidance system, and the risk correlation of the surrounding vehicles was estimated based on the input sensor information applied to the proposed E-SVDD algorithm. The E-SVDD algorithm was implemented with logic B based on the estimated risk correlation index. A basic warning without the E-SVDD algorithm (i.e., pure logic) was also used to compare with the performance of the improved warning system.

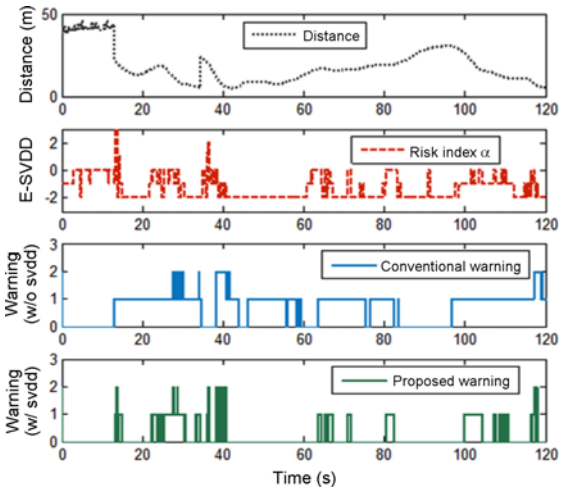

Figure 9. Warnings from each individual logic for highway driving.

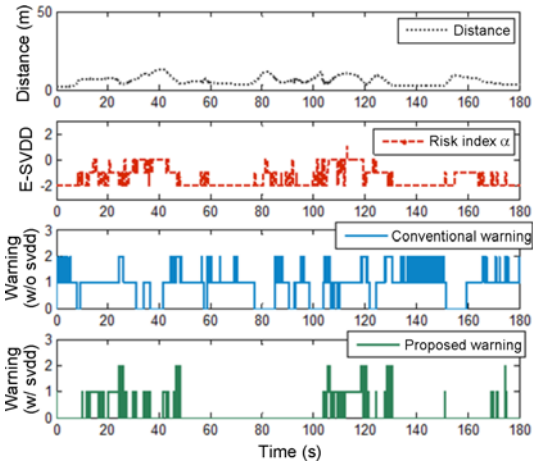

Figure 10. Warnings from each individual logic for urban driving.

Figure 9 shows the numerical simulation of the various warning logics based on actual driving data for a highway.

The intelligent logic inhibited many unnecessary warnings from the conventional logic B. The intelligent logic provided a higher level of warning than the conventional logic around 12 s, and only the intelligent logic provided a warning around 35 s. Both cases occurred when surrounding vehicles tried to change lanes and decelerate. In these situations, the risk is sharply increased according to the E-SVDD algorithm. Figure 10 shows the numerical simulation of various warning logics based on actual urban driving data.

Warnings were more frequent than for driving on a highway. This means that urban driving involves shorter distances between vehicles and more frequent vehicle movement. Nevertheless, frequent warnings while a steady clearance distance is kept between vehicles during urban driving can be regarded as unnecessary by drivers.

The intelligent logic with the E-SVDD algorithm clearly inhibited warnings relative to the conventional logic B. Warnings were mainly given when dangerous situations appeared to occur, such as the deceleration in a short distance or changing of lanes by the target vehicle (Yang, 2012).

5. VERIFICATION

The National Highway Traffic Safety Administration (NHTSA) of the USA. has recommended warning times before collision for deceleration and constant speed tests. This section presents a comparison of the warning times by the conventional logic B and the proposed logic with the NHTSA warning times. Figure 11 shows the warning times from each logic using actual highway driving data.

NHTSA recommends warning times of 2 and 2.4 s before collision for the constant and deceleration tests, respectively (Lee and Peng, 2005; Brunson *et al*., 2002).

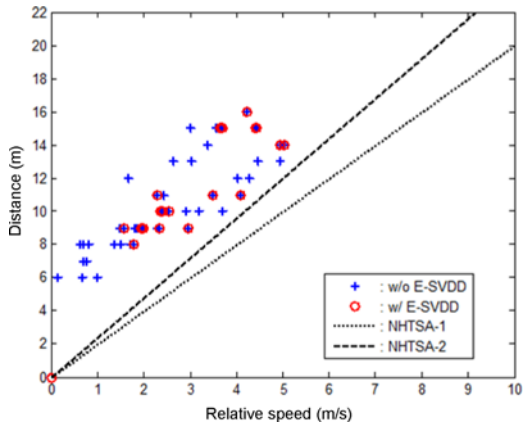

Figure 11. Comparison of warnings from various logics for highway driving.

Unlike logic B, the intelligent logic added warnings based on the conditions of the nearby vehicles; however, it mostly suppressed warnings based on the traffic conditions. Figure 11 shows the results of the highway driving test. Logic B gave 257 warnings, while the intelligent logic gave 70 warnings based on a sampling time of 0.02 s. Thus, the intelligent logic suppressed 72.7 % of the warnings of logic B.

Figure 12 shows the results of the urban driving test. Logic B gave an excessively frequent 749 warnings based on a sampling time of 0.02 s over 180 s. However, the intelligent logic gave 196 warnings. Thus, the intelligent logic suppressed about 73.8 % of the warnings of logic B.

The proposed intelligent logic was confirmed to suppress unnecessary warnings through risk correlation when the behavior of the surrounding vehicles was relatively safe.

The proposed intelligent logic with E-SVDD effectively suppressed 73 % of the unnecessary warnings in the low risk region. In addition, this logic provided proper warnings by controlling the risk correlation when preceding and surrounding vehicles were overtaking and changing lanes.

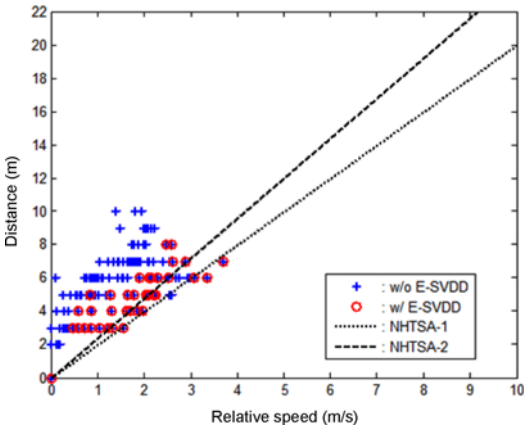

Figure 12. Comparison of warnings from various logics for urban driving.

6. CONCLUSION

An intelligent situation prediction algorithm for a large number of objects with a certain directivity exposed to irregular disturbances was applied to the collision avoidance system logic of driving vehicles.

A new theory called E-SVDD, which is an extension of SVDD, was proposed. A new collision avoidance system logic based on E-SVDD was designed. The performance and effectiveness of the proposed collision avoidance logic were compared with a conventional logic, and it was found to have the following advantages.

(1) It reduces the frequency of unnecessary alerts when the vehicle is cruising on a highway.
(2) It can flexibly cope with sudden situations such as a vehicle cutting in the lane.
(3) Because it predicts the situation by using signals from sensors such as radar, it can potentially be combined with other sensors for multiple purposes.

The following complementary problems should be considered in future studies.

(1) Wider and more varied applications of E-SVDD should be studied.
(2) An algorithm that considers various driver conditions (e.g., elderly, physically disabled) and driving habits (i.e., human factors) is also very important.
(3) An optimization problem to realize E-SVDD in real-time should be studied.

REFERENCES

Blum, J. and Eskandarian, A. (2002). Software architecture for adaptive collision avoidance systems. *Int. J. Automotive Technology* **3**, **2**, 79–88.

Brunson, S. J., Kyle, E. M., Phamdo, N. C. and Preziotti, G. R. (2002). Alert Algorithm Development Program: NHTSA Rear-end Collision Alert Algorithm (No. HS-809 526).

Butsuen, T., Niibe, T., Takagi, T., Yamamoto, Y. and Seni, H. (1994). Development of a rear-end collision avoidance system with automatic brake control. *JSAE Review* **15**, **4**, 335–340.

Duda, R. O., Hart, P. E. and Stork, D. G. (2012). *Pattern Classification*. John Wiley & Sons. New York, USA.

Han, I. (2013). Fuzzy estimation of vehicle speed in pedestrian collision accidents. *Int. J. Automotive Technology* **14**, **3**, 385–393.

Jansson, J. (2004). Dealing with uncertainty in automotive collision avoidance. *Advanced Microsystems for Automotive Applications 2004*. Springer Berlin Heidelberg. New York, USA, 165–180.

Jeong, S. H., Lee, J. E., Choi, S. U., Oh, J. N. and Lee, K. H. (2012). Technology analysis and low-cost design of automotive radar for adaptive cruise control system. *Int.*

J. Automotive Technology **13**, **7**, 1133−1140.

Jung, H. G., Cho, Y. H. and Kim, J. (2010). ISRSS: Integrated side/rear safety system. *Int. J. Automotive Technology* **11**, **4**, 541−553.

Lee, K. and Peng, H. (2005). Evaluation of automotive forward collision warning and collision avoidance algorithms. *Vehicle System Dynamics* **43**, **10**, 735−751.

Na, S., Yang, I. and Heo, H. (2014). Abnormality detection via SVDD technique of motor-generator system in HEV. *Int. J. Automotive Technology* **15**, **4**, 637−643.

Oh, C., Kang, Y. S., Youn, Y. and Konosu, A. (2008). Development of probabilistic pedestrian fatality model for characterizing pedestrian-vehicle collisions. *Int. J. Automotive Technology* **9**, **2**, 191−196.

Oh, C., Kang, Y. S. and Youn, Y. (2009). Evaluation of a brake assistance system (BAS) using an injury severity prediction model for pedestrians. *Int. J. Automotive Technology* **10**, **5**, 577−582.

Park, J., Kang, D., Kim, J., Kwok, J. T. and Tsang, I. W. (2007). SVDD-based pattern denoising. *Neural Computation* **19**, **7**, 1919−1938.

Park, J. and Leem, C. H. (2003). Support vector learning for abnormality detection problems. *J. Korean Institute of Intelligent Systems* **13**, **3**, 266−274.

Prosser, S. J. (2007). Automotive sensors: Past, present and future. *J. Physics: Conf. Series* **76**, **1**, 012001.

Schneider, M. (2005). Automotive radar – Status and trends. *German Microwave Conf*., 144−147.

Seiler, P., Song, B. and Hedrick, J. K. (1998). Development of a collision avoidance system. *Development*, **4**, 17−22.

Tax, D. M. and Duin, R. P. (2004). Support vector data description. *Machine Learning* **54**, **1**, 45−66.

Wikipedia (2013). Cauchy Distribution. http://en.wikipedia.org/wiki/Cauchy_distribution

Yang, I. (2012). *A Study on Intelligent Algorithm for Situation Prediction and Its Application to Automotive Collision Avoidance System*. Ph. D. Dissertation. Korea University. Seoul, Korea.

Ypma, A., Tax, D. M. J. and Duin, R. P. W. (1999). Robust machine fault detection with independent component analysis and support vector data description. *Neural Networks for Signal Processing*, **9**, 67−76.